Int. J. Heat Mass Transfer. Vol. 24, No. 8, pp. 1405–1411, 1981.
Printed in Great Britain

0017-9310/81/081405-07 $02.00/0
Pergamon Press Ltd.

AXIAL THERMAL DISPERSION AND PARTICLE TO FLUID TRANSFER IN PACKED-FLUIDIZED BEDS

D. J. GUNN and P. V. NARAYANAN
Department of Chemical Engineering, University College of Swansea, Singleton Park, Swansea SA2 8PP, U.K.

(*Received* 11 *December* 1980 *and in revised form* 26 *February* 1981)

Abstract—In a packed-fluidized bed small particles are fluidized in the interstices of large particles. The dynamic responses of three packed-fluidized beds have been analysed within the large particle Reynolds number range from 50 to 300; both pulse response and experimental frequency response were recorded. A theory previously given has been used to analyse the experimental responses in terms of the coefficient of thermal dispersion, particle to fluid heat transfer coefficient and intraparticle thermal conductivity; the parameters have been found from the experimental responses by nonlinear regression.

The principal reason for the good thermal properties of the bed appears to be due to a large increase in thermal dispersion within the bed because of the fluidised particles. Intraparticle thermal conductivities found from the responses agreed with probable true values, and particle to fluid heat transfer coefficients were similar to those found for fixed and fluidized beds.

NOMENCLATURE

D,	intraparticle thermal conductivity;
D_f,	fluid thermal conductivity;
D_L,	coefficient of axial thermal dispersion;
d,	particle diameter (large);
G,	rate of conduction into a single particle following a step change;
$\hat{G}$,	Fourier transform of the rate of conduction;
h,	particle to fluid heat transfer coefficient;
K_f,	volumetric heat capacity of fluid;
N,	rate of conduction into a single particle;
Nu,	Nusselt group $= hd/D_f$;
p, q,	quantities defined in [10];
Re,	Reynolds number $dU\rho/\mu$;
T,	envelope or fluid temperature;
$\hat{T}$,	Fourier transform of T;
T_0,	entrance temperature;
t,	time;
U,	superficial velocity;
V,	interstitial velocity;
w,	frequency;
X, X_0, Y, Y_0,	defined by equation (11);
z,	axial coordinate.

Greek symbols

θ, σ, γ,	parameters defined by equations (7)–(9);
η,	bed porosity;
ρ,	fluid density;
μ,	fluid viscosity.

INTRODUCTION

PACKED-FLUIDIZED beds are used in chemical reactors for two principal but different applications. When large catalyst particles or solid to be reacted are placed in a tube to provide or remove heat at the wall, heat transfer from particles to the tube wall may be so limiting that there exists substantial temperature gradients across the tube. If smaller particles are now added to the tube so that small particles are fluidized in the interstices of larger particles, then it has been found that radial temperature gradients are reduced. Such a reduction will allow better temperature control of the solid while processing, so that there are potential improvements of product quality and heat conservation. The small particles may be inert in the process, or in some applications may be of the same material as the larger particles.

The second application arises from the mixing characteristics of fluidized beds and is concerned with a gas phase reaction catalysed by fine solid that is fluidized. In an unrestricted fluidized bed axial mixing of solids and gas is very large so that low conversion of reactant in the gas phase may be experienced, particularly when the fluidized solids are fine. If fluidization is carried out in a tube in which large particles are placed, axial mixing of solid and gas is reduced so that there is an important potential increase in reactant conversion in the gas phase.

The design of such processing units requires a good knowledge of particle to fluid heat transfer, and several investigations have been concerned with the measurement of radial transfer rates and fluid bulk temperatures. Ziegler and Brazelton [1] fluidized glass ballotini in the interstices of brass cylinders and steel spheres, and found that effective radial conductivities were several times greater than conductivities without fluidized ballotini. In a later paper they found that cylindrical packings gave greater thermal conductance than spherical packings [2]. Sutherland *et al.* [3] found that large solid particles reduced wall-to-bed heat transfer in fluidized beds, but screen packings were found to cause little reduction in the maximum heat transfer rates.

Gabor [4] studied axial mixing of solids in packed-fluidized beds in terms of a one-dimensional diffusion

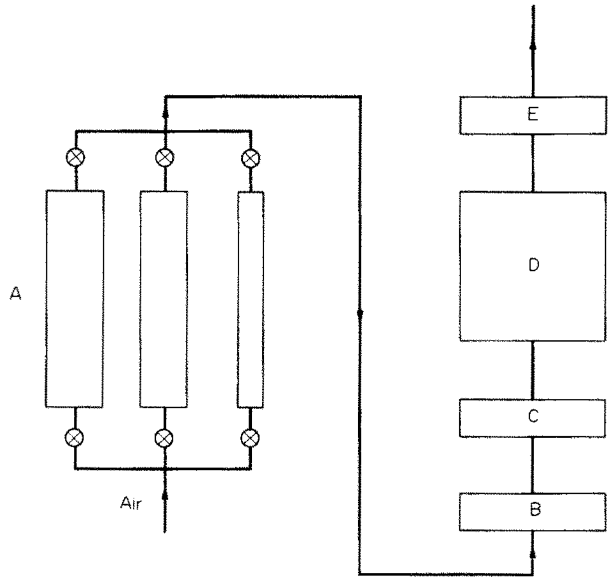

A Flowmeters B, E Temperature sensors
C Gridheater D Test column

FIG. 1. Schematic diagram of the experimental arrangement.

equation and reported values of solids diffusivity for axial mixing. He found that rates of mixing increased with increase in gas velocity, bed height, diameter of packing and column diameter. In a heat transfer study, Gabor, Meecham and Jonke [5] measured rates of heat transfer to beds of large particles in which 100 μm dia. copper shot was fluidized and compared the rates with those obtained from pilot plant fluorination of uranium dioxide pellets. Substantial improvements in heat transfer were obtained with the packed-fluidized bed arrangement.

Such work has established that substantial improvements in rates of heat transfer may be obtained with packed-fluidized beds compared to packed beds. However, the experimental methods that have been used, and the theory behind the experiments have been directed to the estimation of overall heat transfer coefficients from wall to fluid, or to the estimation of effective radial thermal conductivity; axial thermal effects have been ignored. With an incorrect or incomplete model for the transfer process values of transfer coefficients or conductivities that have been estimated include the effect of unconsidered transfer processes and may be far too inaccurate if applied to systems different from that employed in the experimental investigation, even if, for example, just the ratio of length to diameter of tube is changed. A spectacular example of this type of error is shown by published estimates of particle to fluid heat transfer coefficients in packed beds, for which the neglect of axial thermal dispersion can mean order of magnitude differences in heat transfer coefficients [6, 7].

The purpose of the investigation reported in this paper was to measure axial thermal dispersion, particle–fluid heat transfer coefficients and intraparticle thermal conductivity for fixed particles in packed-fluidized beds. The dynamic response is affected by physical properties and transfer processes in the bed that may have no influence in an equivalent steady-state experiment so that more information concerning the viability of the model can usually be obtained from dynamic response.

EXPERIMENTAL ARRANGEMENT

A schematic diagram of the experimental arrangement is shown as Fig. 1. Compressed air at 30 psig was reduced in pressure, filtered and metered by one of a bank of calibrated rotameters. The air passed through a packed distributor section, over the inlet temperature sensor that consisted of a length of platinum wire 0.025 mm in dia. forming one arm of a resistance bridge, over a heater grid and into the experimental column. A wooden conical section was secured to the outlet of the column, and the outlet temperature sensor that formed another arm of the resistance bridge, was placed over the exit slit from this section.

Two experimental columns were used, each made of Perspex 88 mm in dia., and 50 and 80 mm long. The columns were fitted with Tufnol flanges and secured by tie bars. A porous plastic distribution disc 3 mm in thickness was fixed in the base of each column.

Both pulse and sinusoidal input signals were provided at the inlet of the bed by supplying voltages of the appropriate wave form to a grid heater. The power

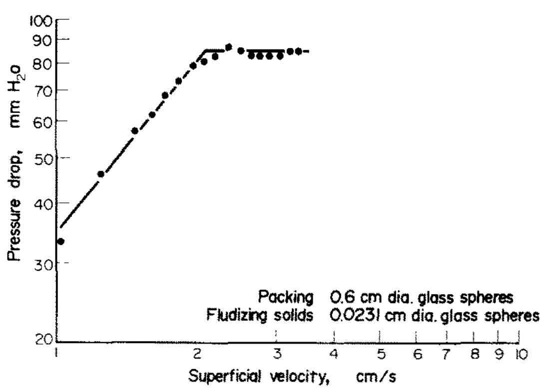

FIG. 2. Dependence of bed pressure drop upon velocity for 6 mm glass and 230 μm glass.

supply unit was originally constructed by de Souza [8]. The arm on a circular, multiposition switch was driven by an electric motor; individual circuits connected to the switch points altered the firing angle of a thyristor-controlled circuit so that a different voltage was delivered to the grid heater as each circuit was connected by the wiper arm. The circuits were arranged to deliver a sequence of voltages to the heater that varied sinusoidally with time. A pulse could be delivered to the grid heater by driving the potentiometer wiper arm to an appropriate position and switching off the driving motor; a pulse interval timer was then used to control the width of the pulse delivered to the grid heater.

The inlet and outlet temperature sensors were made from platinum wire 0.025 mm in dia. wound over a rectangular Tufnol frame so that a slit 30 mm long and 10 mm wide was spanned by the wire wound to a resistance of about 40 Ω. The sensors were placed in a resistance bridge balanced by wire-wound manganin resistors so that there was no resulting voltage without an input to the grid heater; the output voltage was produced because of an out-of-balance condition between the inlet and outlet temperature sensors caused by a change in temperature of the gas passing over the outlet sensor.

Experiments were carried out to obtain two sets of response curves that could be used for analysis by means of a theoretical model.

The two columns 50 and 80 mm in length were packed with the larger particles of the fixed packing, and the 50 mm column was mounted above the grid heater. The desired air flow was set and fine particles were added to the bed until they fluidized in the interstices of the packing to the top of the bed. The temperature sensor was then mounted on the top of the column.

Both pulse and frequency response experiments were carried out.

When the flow was steady preliminary test runs were carried out to obtain the best possible combination of pulse time, recorder sensitivity and chart speed so that the response pulse was of good form. When flow rates and instrumental readings had settled, two pulses were recorded from the column under the same conditions. The 50 mm column was then replaced by the 80 mm column and the above procedure was repeated exactly for the same conditions of flow, pulse time, recorder sensitivity and chart speed.

The set of procedures was repeated for a range of flow rates for different fixed and fluidized packings. The amount of fluidized solids added to the bed was adjusted for each flow rate. The timing of the pulse was usually set at 30 s.

For direct frequency response experiments the timer circuit was disconnected and the wave generator was connected to the mains through an A.C. mains stabiliser.

Three packed-fluidized systems were investigated. In the first lead glass ballotini 230 μm dia. were fluidized in the interstices of 6 mm dia. soda glass spheres. The minimum fluidized velocity was determined from pressure drop measurements; a graph of pressure drop against velocity is shown in Fig. 2. In the second system lead particles of average diameter 196 μm were fluidized in the interstices of 6 mm dia. soda glass spheres and in the third system the 230 μm glass ballotini were fluidized in the interstices of 7.3 mm dia. nickel particles.

Preliminary experiments were performed to find the appropriate frequency ranges for each flow rate so that the output wave was of good form. The wave generator was then set at the chosen frequency and the experiment continued until steady oscillations of temperature were observed on the chart recorder that measured the output from the resistance bridge. Once achieved, about six cycles were recorded, and the average amplitude was calculated. The experiment was repeated for the 80 mm bed and several frequencies.

THEORY OF DISPERSION IN BEDS OF PARTICLES WITH INTRAPARTICLE CONDUCTION

In the packed-fluidized bed a travelling temperature wave causes heat transfer between fluid particles, thermal dispersion and intraparticle conduction. Thermal dispersion is due to molecular conduction in fluid and solid both in the same direction and against the direction of flow, dispersion by velocity difference, mainly in the direction of fluid flow, and in the packed-fluidized bed by circulation currents of fine solids in the interstices of large-diameter packing.

When the circulation currents of solid are large as in the unrestricted fluidized bed, the reflection of currents at the upper surface of the bed will set the free surface boundary condition to be $\partial T/\partial z = 0$, but as the major circulation currents of solid in the packed-fluidized bed are restricted to the interstices of the packing, the appropriate boundary conditions are the semi-infinite set [6]. In the experimental investigation the semi-infinite set gave better agreement with the experimental results as has also been found for experiments on dispersion in packed beds [6, 9].

The partial differential equation that describes adiabatic heat dispersion and transfer in the bed may be written as [10]

$$D_L \frac{\partial^2 T}{\partial z^2} - K_f V \frac{\partial T}{\partial z} - N \frac{1-\eta}{\eta} \phi - K_f \frac{\partial T}{\partial t} = 0. \quad (1)$$

The theoretical foundations of this equation have been described earlier. The rate of conduction N may be related to the envelope temperature T by a variant of Duhamel's theorem [10]

$$N = \int_0^t T(\lambda) \frac{\partial}{\partial t} G(t-\lambda)\, d\lambda \quad (2)$$

where $G(t)$ is the rate of conduction into a medium that is found when the temperature at the surface of a medium initially at zero temperature is raised to unity. Equation (1) then becomes

$$D_L \frac{\partial^2 T}{\partial z^2} - K_f V \frac{\partial T}{\partial z} - \phi \frac{1-\eta}{\eta} \times \int_0^t T(\lambda) \frac{\partial}{\partial t} G(t-\lambda)\, d\lambda - K_f \frac{\partial T}{\partial t} = 0. \quad (3)$$

The boundary conditions are $T = T_0$ at $z = 0$, $T \to 0$ as $z \to \infty$.

At the lower fluid velocities required by the investigation a satisfactory pulse response could not be obtained, but the experimental frequency response could be measured so that frequency response was measured at the lower velocities and pulse response was measured at the higher velocity.

The theoretical frequency response may be found by taking the Fourier transform of equation (3) where the transform is defined

$$F(w) = \hat{T} = \int_0^\infty e^{iwt}\, T(t)\, dt. \quad (4)$$

The equation after transformation becomes

$$\frac{d^2\hat{T}}{dz^2} - \frac{K_f V}{D_L}\frac{d\hat{T}}{dz} - \left(\phi \frac{1-\eta}{\eta D_L} \hat{G} + \frac{iwK_f}{D_L}\right)\hat{T} = 0. \quad (5)$$

The solution is

$$\hat{T} = \hat{T}_0 \exp\left[\left(\frac{K_f V}{2D_L} - \theta\sigma\right) z - i\theta z\right] \quad (6)$$

where

$$\theta = \left[\frac{K_f^2 V^2}{8D_L^2} + \frac{p}{2D_L}\right]^{1/2} \left[\sqrt{(1+\gamma^2)} - 1\right]^{1/2} \quad (7)$$

$$\sigma = \left[\frac{\sqrt{(1+\gamma^2)} + 1}{\sqrt{(1+\gamma^2)} - 1}\right]^{1/2} \quad (8)$$

$$\gamma = \frac{4D_L(q + wK_f)}{K_f^2 V^2 + 4p D_L}. \quad (9)$$

The variables p and q are defined by the shapes and boundary conditions for the particle; expressions defining p and q have been given for a variety of particles [10].

The analysis was based upon the transform $\hat{T}/\hat{T}_0$ that may be calculated from the experimental pulse response by setting e^{-iwt} to $(\cos wt - i \sin wt)$ in equation (4) to give

$$\frac{\hat{T}}{\hat{T}_0} = \frac{\int_0^\infty T \cos wt\, dt - i \int_0^\infty T \sin wt\, dt}{\int_0^\infty T_0 \cos wt\, dt - i \int_0^\infty T_0 \sin wt\, dt}. \quad (10)$$

On setting

$$Y = \int_0^\infty T \cos wt\, dt, \quad X = \int_0^\infty T \sin wt\, dt, \quad Y_0 = \int_0^\infty T_0 \cos wt\, dt, \quad X_0 = \int_0^\infty T_0 \sin wt\, dt \quad (11)$$

the transform ratio is found to be

$$\frac{\hat{T}}{\hat{T}_0} = \frac{(Y Y_0 + X X_0) - i(Y_0 X - Y X_0)}{Y_0^2 + X_0^2}. \quad (12)$$

The attenuation of an input wave may be found from the experimental response by taking the modulus of the complex number [12]. The experimental estimates of attenuation ratio were then compared with the theoretical attenuation ratio of equation (6), and values of the parameter D_L, h and D were changed in a computer program until the experimental points showed minimum variances about equation (6). The values of h, p, D_L associated with the minimum variance were the best values provided by that experiment.

The values so found for each experiment were calculated in the form of axial Peclet group Vd/D_L, Nusselt group hd/D_f and intraparticle thermal conductivity D, and expressed as functions of particle Reynolds number.

DISCUSSION

Validity of the mathematical model

The variances obtained by the frequency response analysis, and by frequency response calculated from pulse response were of similar orders of magnitude so that the variances from both types of experiment formed a homogeneous population. A small overlap in Reynolds number range was arranged so that the experimental frequency response and pulse response were measured at similar Reynolds numbers although the bulk of the frequency response experiments were carried out at lower Reynolds numbers and the bulk of the pulse response experiments were carried out at higher Reynolds numbers. In the region of overlap estimates of parameters from the two methods were similar. Experiments in pulse response carried out at lower Reynolds numbers were not as sensitive to the values of Peclet group, Nusselt group and intraparticle thermal conductivity, as experimental frequency response. The sensitivity of pulse response improved at higher Reynolds numbers and as pulse response was quicker, these experiments were favoured at high Reynolds numbers. The greater sensitivity of experimental frequency response was also found in experi-

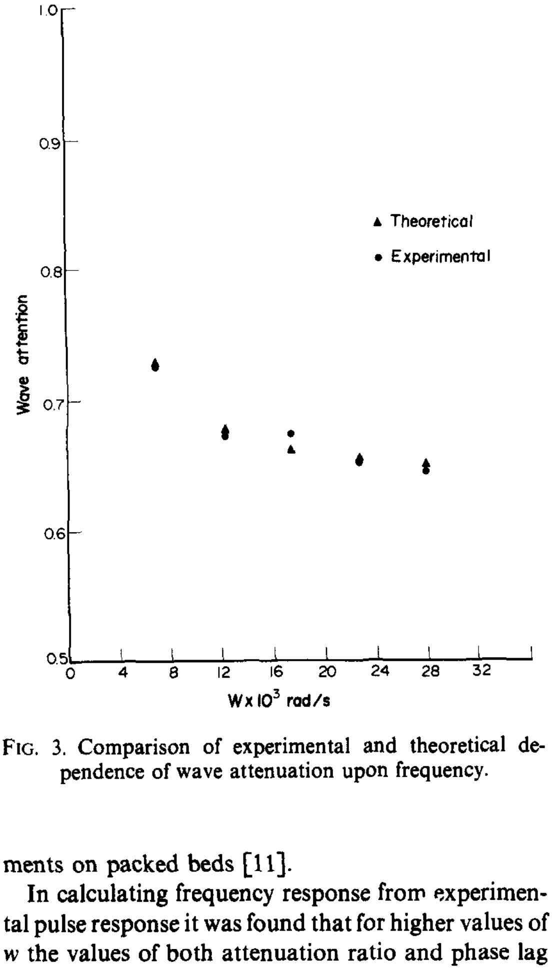

FIG. 3. Comparison of experimental and theoretical dependence of wave attenuation upon frequency.

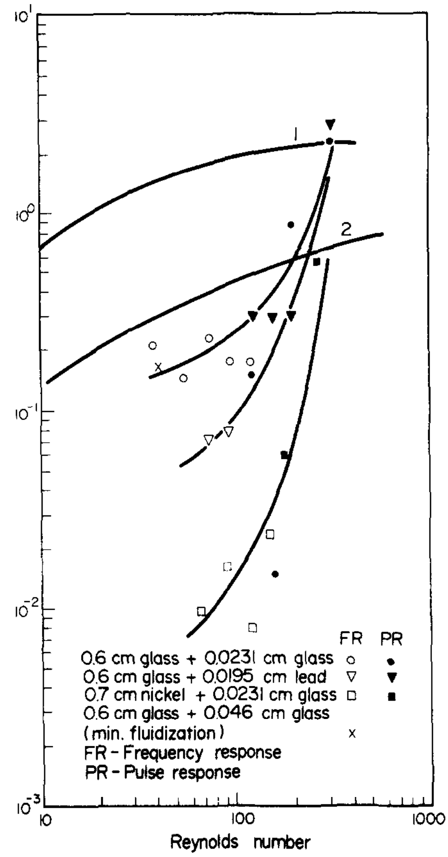

FIG. 4. Dependence of Peclet group upon Reynolds number for different systems.

ments on packed beds [11].

In calculating frequency response from experimental pulse response it was found that for higher values of w the values of both attenuation ratio and phase lag became very erratic. This was more severe in the case of phase lag and therefore the experimental variance was based entirely upon attenuation ratio. The range of w was restricted so that the attenuation ratio did not include a large random component. This behavior was also found in experiments on packed beds [11].

For the particular ranges of application the variance of the experimental points about the theoretical was similar for the experiments on frequency response, and on pulse response. A typical comparison of the dependence of wave attenuation ratio upon frequency is shown in Fig. 3. The average variance of 4.6×10^{-4} was similar to the average value found for closely related experiments on fixed beds at 3.4×10^{-4}— an application of the variance ratio test [12] for 18 and 12 degrees-of-freedom gave a significance level >0.2. It therefore appeared that the model gave an adequate representation of the dependence of attenuation ratio upon frequency since it has been previously established that the model gives a good representation of thermal dispersion in fixed beds [6, 9].

EXPERIMENTAL RESULTS

Axial thermal dispersion

The thermal Peclet groups for axial dispersion are shown in Fig. 4 as functions of Reynolds number for the three different systems. The upper line on the graph marked 1 represents the experimental results of de Souza [6] for fixed beds packed with glass particles. As the Reynolds number is increased the Peclet group for 6 mm glass ballotini with 230 μm glass particles fluidized in the interstices approaches the relationship found for the fixed bed. A similar approach to the fixed bed relationship is shown for 6 mm ballotini with 196 μm lead particles fluidized in the interstices. The fixed bed relationship is reached when the fine solids content of the bed is so low that the thermal characteristics are not affected by the fine particles.

The experimental values of Peclet group for a bed of 7 mm dia. nickel particles with 230 μm ballotini fluidized in the interstices are also shown on the figure. As the Reynolds number is increased the Peclet group approaches line 2 on the diagram, the experimental results of de Souza [6] for axial thermal dispersion in beds of metallic particles.

A single experimental measurement of thermal dispersion in a bed of 6 mm glass particles with 460 μm glass ballotini in the interstices is also shown on the figure. This result was taken at minimum fluidization, and it is therefore apparent that there is a sharp reduction in Peclet group after the onset of fluidization. The general pattern is one in which the Peclet group falls rapidly with the onset of fluidization of fine particles in the interstices of large particles. As the

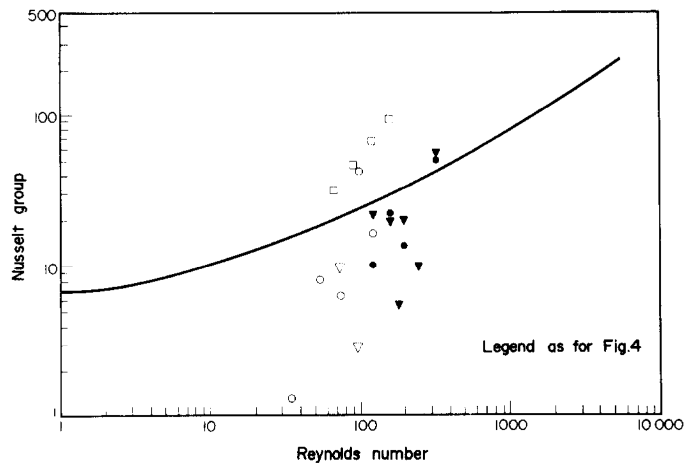

FIG. 5. Comparison of experimental Nusselt groups with equation (13).

velocity is increased beyond this point the Peclet group increases until the fixed bed relationship is approached when the fine particles have been substantially removed from the bed. Coefficients of thermal dispersion when the fine particle concentration is relatively high are about 20 to 30 times larger than fixed bed values. The increase in thermal dispersion is large enough to give a substantial improvement in temperature control for a practical chemical reactor. The effect is particularly strong if the fine particles are metallic.

Intraparticle thermal conductivity

Although intraparticle temperature gradients may be different from zero in the fine particles, the effect will be slight because the particles are so small. However intraparticle gradients may well be significant in the larger fixed packing so that the effect of intraparticle conduction was included in the theory, and estimated from the experimental results.

For metallic fixed packing the experimental results in the neighbourhood of the best fitted curve, showed that the thermal conductivity was large, but a precise estimate could not be made because of the insensitivity of the theoretical response to variations in the intraparticle conductivity.

The mean value of the thermal conductivity of the 6 mm soda glass particles found from experiments in which lead glass ballotini was fluidized in the interstices, was 2.31×10^{-3} cal/cm s K with a standard deviation of 0.32×10^{-3} cal/cm s K. The mean value for the fixed packing found from experiments in which lead shot was fluidized in the interstices was 2.63 with a standard deviation of 0.22×10^{-3} cal cm s K. The estimates agree with each other and with values reported in the literature for soda glass.

Fluid–large-particle heat transfer

The minimum variance analysis of the experimental results also provided estimates of the fluid–fixed-particle heat transfer coefficient, that was expressed as the dependence of particle Nusselt group upon Reynolds number. This dependence has been plotted in Fig. 5.

The full line in the figure represents an equation that has been previously given for the dependence of Nusselt group upon Reynolds number for both fixed and fluidized beds. It is [7]

$$Nu = (7-10\eta+5\eta^2)(1+0.7\,Re^{0.2}\,Pr^{1/3}) + (1.33-2.4e+1.2e^2)\,Re^{0.7}\,Pr^{1/3}\ldots \quad (13)$$

There is a scatter of points about the line in the narrow Reynolds number range of the investigation. However, inspection of the points shows that the scatter is random without an apparent systematic effect so that equation (13) is indeed representative of particle-to-fluid heat transfer coefficients for fixed particles in fixed-fluidized beds. A similar scatter of reported results is found for fixed beds [6, 9], but for unrestricted fluidized beds the variation is much less than shown in the figure. It is probable that the principal reason for the scatter is the uncertainty in finding three parameters from experimental data that are contaminated by error.

However the experimental estimates of Nusselt group are consistent with estimates for similar systems, and this consistency together with the agreement of intraparticle thermal conductivity with probable true values is a further confirmation of the validity of the model. Of the physical factors considered in this experimental programme it appears that the increase of thermal dispersion due to fluidization of fine particles in the interstices of large particles is the principal reason for the good thermal properties of fixed-fluidized beds.

Acknowledgements—The authors wish to acknowledge a research studentship for P. V. Narayanan in the University College of Swansea provided by courtesy of Professor J. F. Richardson of the Department of Chemical Engineering.

REFERENCES

1. E. N. Ziegler and W. T. Brazelton, *Ind. Engng Chem. Proc. Des. Dev.* **2**, 276–281 (1963).
2. E. N. Ziegler, R. W. Frischmalti and W. T. Brazelton, *Ind. Engng Chem. Proc. Des. Dev.* **4**, 239–240 (1965).
3. J. P. Sutherland, G. Vassilatos, H. Kubota and G. L. Osberg, *A.I.Ch.E. Jl* **9**, 437–441 (1963).
4. J. D. Gabor, *Chem. Engng Prog. Symp. Ser.* **62**, No. 67, 35–41 (1966).
5. J. D. Gabor, W. J. Meecham and A. A. Jonke, *Chem. Engng Prog. Symp. Ser.* **60**, No. 47, 96–104 (1964).
6. D. J. Gunn and J. F. C. de Souza, *Chem. Engng Sci.* **29**, 1363–1371 (1974).
7. D. J. Gunn, *Int. J. Heat Mass Transfer* **21**, 467–476 (1978).
8. J. F. C. de Souza, Ph.D. Thesis, University of Wales (1969).
9. D. J. Gunn, P. V. Narayanan and A. P. Wardle, *Proc. Sixth Int. Heat Transfer Conf.*, Montreal, p. 14 (1978).
10. D. J. Gunn, *Chem. Engng Sci.* **25**, 53–66 (1970).
11. H. Y. Bashi and D. J. Gunn, *A.I.Ch.E. Jl* **23**, 40–48 (1977).
12. K. A. Brownlee, *Industrial Experimentation* 4th ed. H.M.S.O., London (1949).

DISPERSION THERMIQUE AXIALE ET TRANSFERT ENTRE PARTICULE ET FLUIDE DANS LITS FIXES–FLUIDISES

Résumé — Dans un lit fixé–fluidisé des petites particules sont fluidisés dans les interstices des grosses particules. Les réponses dynamiques de trois lits fixes–fluidisés ont été analysées pour un domaine de nombre de Reynolds entre 50 et 300 pour les grosses particules ; on a enregistré la réponse en impulsion et en fréquence. Une théorie antérieurement donnée est utilisée pour analyser les réponses expérimentales en fonction de transfert entre particule et fluide et de la conductivité thermique intraparticulaire ; les pâramètres sont déduits des réponses expérimentales par une régression non-linéaire. La raison principale des bonnes propriétés thermiques du lit semble être due à un fort acroissement de la dispersion thermique dans le lit à cause des particules fluidisées. Les conductivités thermiques intraparticulaires trouvées à partir des réponses s'accordent avec les valeurs réelles probables et les coefficients de transfert entre particule et fluide sont semblables à ceux trouvés pour des lits fixes ou fluidisés.

AXIALE THERMISCHE AUSBREITUNG UND WÄRMEÜBERGANG VOM TEILCHEN ZUM FLUID IN FEST-FLIESSBETTEN

Zusammenfassung—Ibn einem Fest-Fließbett werden die kleinen Teilchen in den Zwischenräumen der großen Teilchen fluidisiert. Die dynamischen Ganglinien von drei Fest-Fließbetten wurden innerhalb des Reynolds-Zahlbereichs von 50 bis 300, bezogen auf die großen Teilchen, untersucht. Sowohl Impulsantwort als auch Frequenzgang wurden aufgezeichnet. Eine schon früher aufgestellte Theorie wurde herangezogen, um die experimentell ermittelten Ganglinien im Hindblick auf ihre Abhängigkeit von der thermischen Ausbreitung, den Wärmeübergangskoeffizienten zwischen Teilchen und Fluid und die Wärmeleitfähigkeit innerhalb des Teilchens zu untersuchen; die Parameter wurden aus den experimentellen Gangkurven durch nichtlineare Regression ermittelt. Der Hauptgrund für die guten thermischen Eigenschaften des Bettes liegt offensichtlich in der Großen Zunahmne der thermischen Ausbreitung innerhalb des Bettes durch die fluidisierten Teilchen. Die Werte für die Wärmeleitfähigkeit innerhalb der Teilchen, die aus den Gangkurven ermittelt wurden, stimmten mit wahrscheinlichen Werten überein, und die Wärmeübergangskoeffizienten zwischen Teilchen und Fluid waren den Werten, die für Fest- und Fließbetten ermittelt wurden, ähnlich.

АКСИАЛЬНАЯ ДИСПЕРСИЯ ТЕПЛА И ТЕПЛОПЕРЕНОС ОТ ЧАСТИЦ К ЖИДКОСТИ В ПЛОТНЫХ ПСЕВДООЖИЖЕННЫХ СЛОЯХ

Аннотация — В плотном псевдоожиженном слое мелкие частицы «кипят» в зазорах между крупными частицами. Проведен анализ динамических характеристик трех плотных слоев при значениях числа Рейнольдса для крупных частиц в диапазоне от 50 до 300. В экспериментах снимались импульсные и амплитудно-частотные характеристики. В соответствии с ранее предложенной теорией экспериментальные данные описывались с помощью коэффициента дисперсии тепла, коэффициента теплопереноса от частиц к жидкости и теплопроводности частиц. Параметры процесса определялись путем нелинейной регрессии. По-видимому, хорошие тепловые характеристики слоя обязаны в основном существенному увеличению дисперсии тепла за счет псевдоожижения частиц. Полученные значения теплопроводности частиц совпали с предполагаемыми точными значениями. Коэффициенты теплопереноса от частиц к жидкости оказались аналогичными тем, которые были получены для неподвижных и псевдоожиженных слоев.